

# Exploration of Optical Signal QoT Margin with Intelligent WSS Filtering Penalty Estimator Using Neural Network

Tianliang Zhang

*The University of Texas at Dallas*

Richardson, TX, USA

tianliang.zhang@utdallas.edu

Mustafa AL-QADI

*The University of Kansas*

Lawrence, KS, USA

mustafa.alqadi@ku.edu

Rongqing Hui

*The University of Kansas*

Lawrence, KS, USA

hui@ittc.ku.edu

Andrea Fumagalli

*The University of Texas at Dallas*

Richardson, TX, USA

andrea@utdallas.edu

**Abstract**—Deployment of 5G requires increased data transmission capacity in the metro fiber network. Besides deploying new dark fiber operators are also looking into solutions that improve fiber spectrum utilization by means of high-order modulation formats, flexible grid, and subcarrier multiplexing (SCM) technologies. An important factor that limits fiber spectrum utilization in metro network is the penalty inflicted on the optical signals that are routed by wavelength selective switches (WSS). In this paper, an intelligent WSS filtering penalty estimator is proposed based on neural network. With the achieved accuracy of 0.34 dB of mean absolute error in estimating the optical signal-to-noise ratio penalties caused by WSS filtering, the trained neural network is applied to estimate the fiber throughput gains that can be obtained by optimally selecting the signal symbol rate in a number of use cases.

**Index Terms**—optical communication, WSS filtering penalty, neural network, elastic optical networks, subcarrier multiplexing

## I. INTRODUCTION

With the expanding use of 5G and Internet of Things (IoT), the number of Internet users and connected devices is growing rapidly [1]. The demand for higher communication throughput especially in the metro area network (MAN) raises a great deal of concern among network operators. Dense wavelength-division multiplexing (DWDM) optical transport networks have been deployed for decades and their ability to support high data rate transmissions continues to improve. In such networks, higher spectral efficiency (SE) can be realized in three ways: adopting high-order modulation formats, allowing tighter channel spacing with flexible bandwidths, and implementing subcarrier multiplexing (SCM) [2]. First, applying high-order modulation format enables the optical signal to carry more bits per symbol, especially for polarization-multiplexed coherent modulation. However, higher optical-signal-to-noise ratio (OSNR) is required to achieve low bit-error rates (BER). Second, there is increasing interest in moving from traditional fixed-grid DWDM networks (typically with 50-GHz channel spacing) to elastic optical network (EON) with finer channel granularity, such as 12.5 GHz

or 6.25 GHz [3]. Despite the fact that there exists a large theoretical gain in optical capacity with EON, tighter channel spacing brings up additional impairment, mainly from wavelength selective switches (WSS) filtering penalties [4]. Third, SCM has been proven to be an efficient way to mitigate the fiber nonlinearity and WSS filtering impairments [5] [6]. SCM brings new opportunities and challenges in DWDM system design and network planning.

In transparent optical networks, data carried by optical circuits travel from the source node to the destination node through multiple intermediate nodes without requiring optical-electrical-optical conversion. Each node hosts a reconfigurable optical add/drop multiplexer (ROADM) to add, drop, or simply switch through the optical circuit. WSSs are the key components in ROADM nodes which individually route each optical circuit towards the intended destination. The number of WSSs an optical signal must traverse depends on the network path hop count and the chosen ROADM node architecture. In colorless and directionless (CD) ROADMs, two WSSs must be traversed by the signal at the add, drop, and pass-through node. In colorless, directionless, and contentionless (CDC) ROADMs [7], three WSSs must be traversed by the signal at both the add and drop node, and only two at the pass-through node. Signal penalties induced by WSS filtering are typically negligible in conventional 50-GHz grid DWDM networks when using standard symbol rates, such as 28 Gbd and 32 Gbd. However, these penalties become quite relevant in EON as the channel spacing gets tighter [8]. Moreover, with the rise of edge computing and edge storage, MANs are expected to host more ROADM nodes, resulting in network paths with increased hop count and even more significant WSS filtering penalties. Accurately estimating the WSS filtering penalty in these emerging scenarios is therefore of the essence.

In this paper, we present a neural network (NN) solution<sup>1</sup> to estimate the WSS filtering penalty experienced by the routed optical signal in a wide range of cases. Combined features of the optical signal and WSS configuration are chosen to form

This work was supported in part by NSF Grants No. ACI-1541461, CNS-1531039, CNS-1956137, and CNS-1956357

<sup>1</sup>NNs have been successfully applied to modeling complex problems and have been widely adopted in many fields and applications, including optical communications and network [9].

the NN input, including symbol rate, filter bandwidth, signal center frequency relative to the center of the optical filter, signal root-raised-cosine roll-off factor, modulation format, and the number of cascaded WSSs.

The described NN solution circumvents the challenge of having to derive non-straightforward analytical models and/or close formula in order to quickly estimate the WSS filtering penalties in a variety of scenarios. Unlike time consuming physical layer simulation-based or experimental approaches [10], the NN solution produces penalty estimations in sub-second time, typically less than 0.1 s.

Once trained, the NN solution reaches an accuracy of 0.34 dB of mean absolute error in the OSNR penalty estimated value. Thanks to this accuracy and the NN short computation time it is possible to investigate the fiber throughput gains that can be achieved by selecting the optimal symbol rate and SCM configuration that best make use of the available OSNR margin as a function of the path hop count in MAN. Two specific use cases are considered. First, the highest throughput in a flexible symbol rate scenario is found to produce up to 64% gain when compared to the standard fixed symbol rate solution in a typical MAN. Second, the optimal SCM channel configuration is obtained, which is found to produce further throughput gains up to 35%.

## II. WSS FILTERING PENALTY

### A. WSS Transfer Function

The frequency response of a WSS device can be analytically characterized by (1) (2) [11], where  $BW_{OTF}$  is the roll-off factor and  $B$  is the bandwidth of the aperture of the WSS (usually set to match channel spacing). This model shows good agreement with practical WSS device measurements.

$$S(f) = \frac{1}{2}\sigma\sqrt{2\pi} \left[ \operatorname{erf} \left( \frac{\frac{B}{2} - f}{\sqrt{2}\sigma} \right) - \operatorname{erf} \left( \frac{-\frac{B}{2} - f}{\sqrt{2}\sigma} \right) \right]. \quad (1)$$

$$\sigma = \frac{BW_{OTF}}{2\sqrt{2\ln 2}} \quad (2)$$

Cascading multiple WSS devices has the net effect of multiplying their bandpass frequency responses together. Fig. 1 shows the equivalent 6 dB bandwidth after a number of cascaded WSS modules, assuming that the WSS modules have ideal and identical frequency responses.

### B. WSS Filtering Penalty Estimation through Simulation

To estimate the WSS filtering penalty on an optical signal, we built a coherent transmission simulator in MATLAB with (1) (2) implemented to simulate the WSS transfer function. Dual polarization coherent optical transmission with quadrature amplitude modulation (QAM) is considered. The transmitter can be programmed to generate different modulation formats, variable symbol rates, and Nyquist filtering. At the receiver the signal is first matched-filtered, then down-converted to baseband for demodulation and symbol-to-bit mapping for

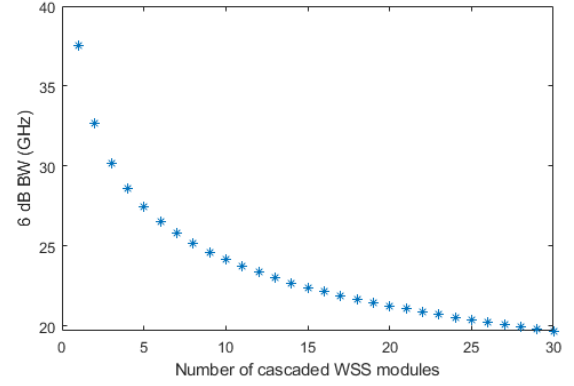


Fig. 1. Equivalent 6 dB bandwidth of cascaded WSS modules, where  $BW_{OTF} = 10.5$  GHz and  $B = 37.5$  GHz.

bit error counting. The digital-to-analog and analog-to-digital converters (DACs/ADCs) in the transmitter and receiver are assumed to have frequency-independent bit resolution of 8. With a 9 sample per symbol resolution each simulation run generates at least  $10^5$  QAM symbols to achieve reliable BER counting.

Fig. 2 shows the WSS filtering OSNR penalty in a 32 Gbd 256 Gbps optical signal modulated as PM-16QAM with 37.5 GHz channel spacing as it is routed through WSS modules. Considering that a minimum of 4 cascaded WSSs are needed to provision an optical circuits between two ROADMs (a single hop path), the resulting OSNR penalty (14.4 dB) quickly becomes prohibitively high. This example shows how the WSS filtering effect can induce significant transmission degradation in EON with narrow channel spacing. Considering that numerical simulation techniques to estimate OSNR penalty for each of the possible link configurations are time consuming, a faster and comprehensive alternative solution is highly desirable in a network controller or planning tool.

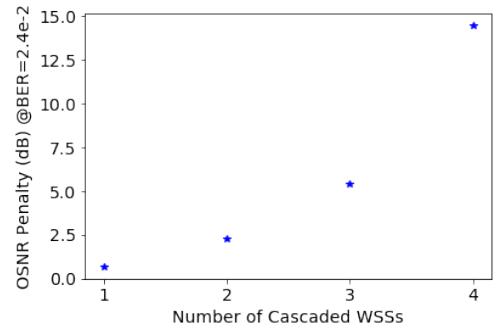


Fig. 2. OSNR penalty for 32 Gbd 256 Gbps optical signal modulated as PM-16QAM with 37.5 GHz channel spacing due to cascaded WSS filtering.

## III. WSS FILTERING PENALTY ESTIMATION THROUGH NN

### A. Introduction on Neural Networks

Neural network (NN) is a group of models with varying structures that can be applied to learn how to solve most

complex numerical problems through an effective input-output variable mapping. Viable structures may vary based on the specific problems under consideration. Typical NN structures include artificial neural networks, convolutional neural networks, and recurrent neural networks. Classification and regression are two typical tasks neural networks are designed for. In this paper, artificial neural network is chosen to model the WSS filtering characteristics and estimate the resulting OSNR penalty through non-linear regression.

A generalized artificial neural network structure is shown in Fig. 3. The input layer contains a number of neurons matching the number of input features. Since the purpose here is to estimate the OSNR penalty corresponding to the applied input features, the output layer contains only one neuron, which provides the computed OSNR. Between the input and output layer, one or more hidden layers are deployed, each hosting a number of neurons. Each neuron is fully connected with the neurons in the previous and successive layers and applies a non-linear activation function to the weighted sum of the incoming values to produce its outgoing value. This NN type is also known as feedforward neural network for supervised learning. The NN training process requires a backpropagation algorithm that calculates the gradient of the loss function with respect to the weights iterating backward from the last layer to the first layer [12].

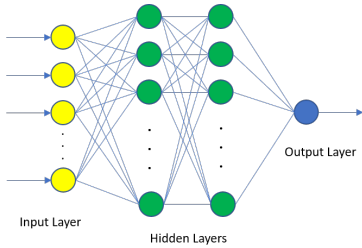


Fig. 3. A generalized artificial neural network structure.

## B. Dataset

Due to insufficient experimental data for WSS filtering penalty available to the authors, the training dataset is generated with the help of the simulator in Section II-B. Features (illustrated in Fig. 4) and restrictions are described next.

- $R_s$ : Symbol rate, is a continuous value from 2 Gbd to 42 Gbd. The 2 Gbd lower limit is set to account for to SCM channels which may use only part of  $B$ . The 42 Gbd upper limit is set to account for most signal width with respect to the 50 GHz upper limit of  $B$ .
- $B$ : WSS filter bandwidth (channel spacing), is a continuous value from  $\max(6.25 \text{ GHz}, R_s)$  to 50 GHz. The minimum nominal central frequency granularity defined by the ITU-T is 6.25 GHz [13]. The upper limit is 50 GHz as it is the grid for traditional fixed grid DWDM network. Other values such as 67.5, 100 GHz, etc. are also acceptable.
- $\Delta f$ : Signal center frequency relative to the center of the optical filter, is a continuous value from  $(-B + R_s)/2$  to

$(B - R_s)/2$  that accounts for all possible relative positions of a SCM channel.

- $\sigma$ : Signal root-raised-cosine roll-off factor, is a continuous value from 0.01 to 1.
- $M$ : Modulation format, is one of the following six categories: PM-BPSK, PM-QPSK, PM-8QAM, PM-16QAM, PM-32QAM, and PM-64QAM.
- $n$ : Number of cascaded WSSs, is a discrete value from 1 to 20.
- $OSNR_{WSS}$ : WSS filtering OSNR penalty, is the output value the neural network needs to make regression on.

By selecting a sufficient number of key features that may affect the WSS filtering penalty, the trained neural network is supposed to be valid in a wide range of uses. Feature values are randomly selected within their respective ranges when generating the training dataset.

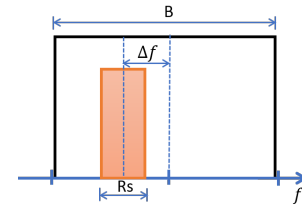


Fig. 4. Parameters used to generate the training dataset.

## C. Pre-processing

Pre-processing of the input features is necessary to increase the NN accuracy. For continuous-valued features,  $R_s$ ,  $B$ ,  $\Delta f$ , and  $\sigma$ , each feature is scaled by its maximum absolute value. For discrete-valued features, values are encoded using binary digits. Three digits are needed for feature  $M$  and five digits are needed for feature  $n$ . A total of 12 features are used.

## D. NN Structure

The input layer contains 12 neurons to account for the 12 features. Two hidden layers, each hosting 256 neurons, are applied. ReLu is used as the activation function of each hidden neuron. ReLu is selected because it causes fewer vanishing gradient problems compared to other activation functions. Based on our preliminary research by trail and compare, we determined that this structure provides a good accuracy.

## E. Training Process and Results

The dataset contains 38,606 training samples and 9,652 validation samples. Samples are shuffled in each epoch. Adam optimizer is used during the training process. The training process is conducted in TensorFlow environment. The mean absolute error is used as performance indicator.

The training and validation error against the training epoch is shown in Fig. 5. The blue curve is training loss/error, and orange is validation loss/error, which are labeled in the legend. The validation error histogram is shown in Fig. 6.

The mean absolute error on the validation set is 0.34 dB, with 92.26% of validation samples falling within 1 dB and

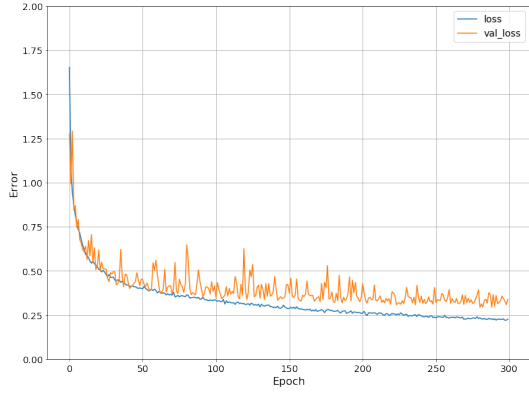


Fig. 5. Training and validation error (dB) over 300 epochs.

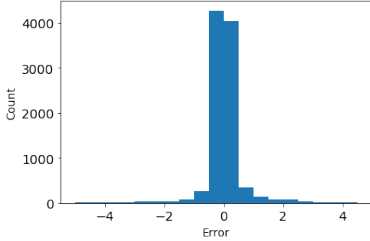


Fig. 6. Validation error (dB) histogram.

85.98% falling within 0.5 dB from the OSNR value obtained from the simulator. We believe this accuracy is sufficient to make realistic predictions on the WSS filtering penalty. Once the NN is trained, it can be deployed in optical network controller, planning tool, simulation, and real-time emulation engines. Improved accuracy can be achieved by further training the neural network with more training samples or experimental data.

The NN runtime to estimate the WSS filtering penalty for one set of feature values is around 0.08 s, which is more than two orders of magnitude faster than getting the estimation from the simulator. The NN short runtime facilitates the two studies discussed in the next section.

#### IV. TWO USE CASES

The OSNR penalty estimated using the NN in Section III only accounts for the presence of the WSS filtering penalties along the circuit path. Additional OSNR penalties may be due to amplified spontaneous emission noise (ASE) from amplifiers and nonlinear interference noise (NLI). These two additional impairments are estimated through the GN model [14] as

$$P_{ASE} = hf_0FB_{ref}(G - 1), \quad (3)$$

and

$$P_{NLI} = P_S^3 \frac{16}{27\pi} \frac{\alpha}{|\beta_2|} \gamma^2 \frac{L_{eff}^2}{R_s^3} B_{ref} \ln\left(\frac{\pi^2}{2} |\beta_2| \frac{R_s^2}{\alpha} \left(\frac{B_{opt}}{B}\right)^2 \frac{R_s}{B}\right), \quad (4)$$

where  $h$  is Plank's constant,  $f_0$  is the center frequency of the C-band,  $F$  is the amplifier noise figure,  $B_{ref}$  is the

resolution bandwidth (RBW) of the OSNR measurement,  $G$  is the amplifier gain,  $P_S$  is the signal power,  $\alpha$  is the fiber attenuation,  $\beta_2$  is the chromatic dispersion coefficient,  $\gamma$  is the nonlinear coefficient,  $L_{eff}$  is the effective fiber length, and  $B_{opt}$  is the occupied bandwidth. For an optical circuit with multiple line spans (LS), the path OSNR is computed as

$$OSNR_{Path} = \left(\sum_{LS,i} \frac{1}{OSNR_{LS,i}}\right)^{-1} \quad (5)$$

$$OSNR_{LS} = \frac{P_S}{P_{ASE} + P_{NLI}}, \quad (6)$$

where  $i$  identifies the LS in the path. Assuming that ASE and NLI are independent of the WSS filtering penalty, the circuit OSNR should satisfy

$$\frac{OSNR_{Path} - OSNR_{WSS}}{OSNR_{receiver} + OSNR_{guard}} > \quad (7)$$

where  $OSNR_{WSS}$  is the WSS filtering penalty after  $4 + (i - 1) \times 2$  cascaded WSSs (CD ROADMs is considered),  $OSNR_{receiver}$  is the OSNR required to achieve the desired low BER at the optical receiver at the destination node, and  $OSNR_{guard}$  is the safety margin, set at 1 dB.

#### A. Flexible Symbol Rate

Conventional transmitter-receiver pairs operate at fixed standard symbol rates, e.g., 28 Gbd or 32 Gbd. Transmission data rates can only be varied by changing the modulation format subject to the available  $OSNR_{receiver}$ . In this section we explore the throughput gain that is achievable by introducing transmitter-receiver pairs that can operate with flexible symbol rates. Throughput is defined as the highest achievable data rate subject to (7). The applied  $OSNR_{receiver}$  accounts for typical SD-FEC BER threshold ( $2.4e^{-2}$ ) and the reported data rates (throughput) include FEC overheads.

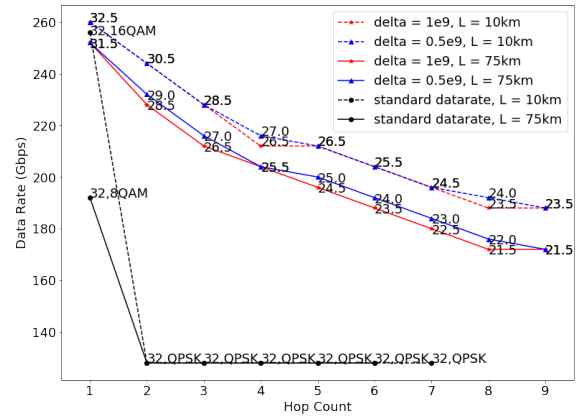


Fig. 7. Throughput of standard fixed symbol rate and flexible symbol rate solutions versus path hop count (CD ROADMs is considered).

Fig. 7 compares the throughput of standard fixed symbol rate solutions against flexible symbol rate solutions as a function of the hop-count of the path routed through CD ROADMs. A single carrier is used per channel and the channel

spacing is set to 37.5 GHz. LSs have equal length which is set to either 10 km (dashed) or 75 km (solid). In the fixed symbol rate solution (black) PM-16QAM is only possible when operating the channel over a single hop with LS length of 10 km. In all other cases up to 7 hop count PM-QPSK must be applied. For higher hop counts the WSS filtering penalties do not allow PM-QPSK to operate successfully. In contrast, PM-16QAM is always used in the flexible symbol rate solution. By adjusting the applied symbol rate this solution can mitigate the penalties induced by the cascaded WSS filters on the transmitted signal. Two symbol rate resolutions are applied when searching for the highest data rate — 0.5 Gbd (blue) or 1 Gbd (red) — starting with the initial symbol rate of  $B$  (37.5 Gbd). Reducing the symbol rate resolution below 1 Gbd does not yield significant throughput gains. Overall the flexible symbol rate solutions are able to yield considerable through gain when compared to the fixed solution. For large hop count ( $>7$ ) the variable symbol rate solution is still able to offer about 180 Gbps while the fixed symbol rate solution cannot even operate with PM-QPSK.

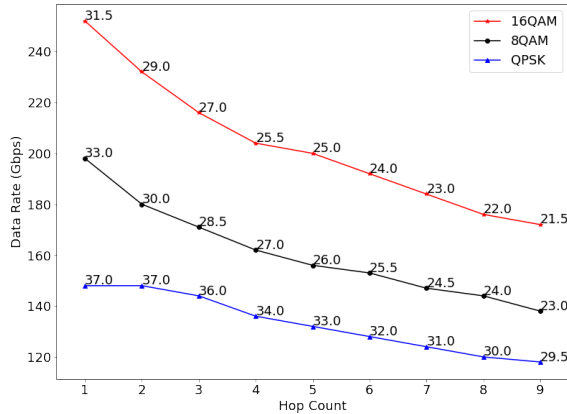


Fig. 8. Throughput comparison between three different modulation formats under flexible symbol rate circumstance.

Fig. 8 reports the throughput of the flexible symbol rate solution for three modulation formats, i.e., PM-QPSK, PM-8QAM and PM-16QAM as a function of the path hop count. These results are obtained assuming LS length of 75 km and symbol rate resolution of 0.5 Gbd. As one would intuitively anticipate, high-order modulation formats are heavily affected when the number of traversed WSS filters increases. Their throughput declines sharply as the hop count increases. Low-order modulation formats on the other hand are able to operate at increased symbol rates even in excess of the 32 Gbd standard fixed value when the hop count is low.

Next, we further investigate the throughput gain in an hypothetical MAN. Fig. 9 shows the network topology of an hypothetical MAN in Toronto city<sup>2</sup> [15]. Between each node pair, two shortest paths are pre-computed [16]. The average throughput for each path group categorized by hop

<sup>2</sup>Span lengths shown in the figure are estimated based on the segment length and city size measured on Google Maps.

count is shown in Fig. 10 for both fixed symbol rate and flexible symbol rate solutions. The two solutions yield similar throughput in single-hop paths. For larger hop counts the flexible symbol rate solution consistently outperforms the standard fixed symbol rate solution, which is forced to operate at the low-level modulation format PM-QPSK. A 64.67% network throughput gain is obtained when using the flexible symbol rate solution.

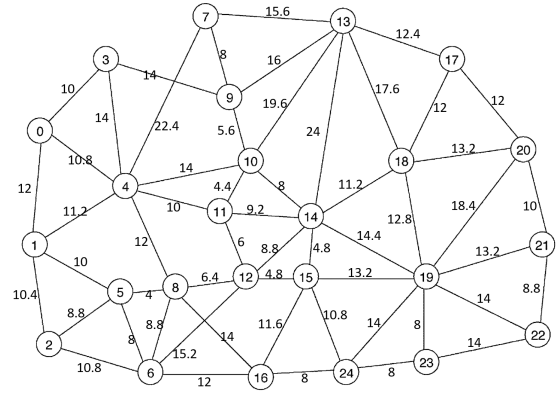


Fig. 9. Toronto-MAN topology (LS length in km).

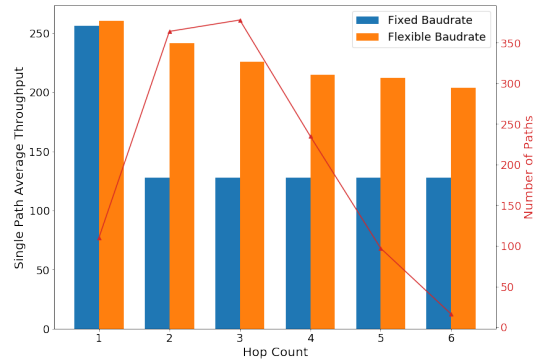


Fig. 10. Average throughput for both flexible (orange) and fixed (blue) symbol rate solutions in the Toronto-MAN.

### B. Best Subcarrier Configuration

The NN in Section III is applied next to estimate the WSS filtering penalties when using multiple subcarriers in the same channel to form a superchannel. The subcarriers that are close to the edge of the WSS filter transfer function are more heavily affected when compared to the subcarriers that are closer to the central frequency of the WSS filter. Consequently, for optimal throughput each subcarrier is individually assigned the highest-order modulation format subject to (7).

Channel spacing is set to 37.5 GHz. When four subcarriers are used, the symbol rate of each subcarrier is 8 Gbd with a guardband of 0.8 GHz between adjacent subcarriers. When eight subcarriers are used, the symbol rate of each subcarrier is 4 Gbd with a guardband of 0.4 GHz between adjacent subcarriers. Fig. 11 reports throughput versus path hop count



for 4 possible scenarios: (green) 8 subcarriers and LS length of 10 km; (yellow) 8 subcarriers and LS length of 75 km; (red) 4 subcarriers and LS length of 10 km; and (blue) 4 subcarriers and LS length of 75 km. Other superchannel configurations are outside the scope of this study. Arrays in the figure report the modulation formats found by the NN for each optimal solution starting with the two innermost subcarriers — closest to the filter central frequency — and ending with the two outermost subcarriers — closest to the filter edge. (Modulation formats are applied symmetrically with respect to the filter central frequency.) For example array [64, 64, 16, 2] applies to 8 subcarriers in which PM-64QAM is used in the two innermost subcarriers and PM-BPSK is used in the outermost subcarrier. In some configurations not all the 8 subcarriers can be established, like in the case of 6 hops and LS length=75 km (yellow). The solution in this case is [32, 32, 4], which indicates that the two outermost subcarriers cannot be successfully operated due to the heavy WSS filtering penalties. In paths with low hop count the 8 subcarrier solutions always outperform the 4 subcarrier solutions regardless of the LS length, with up to 35% of throughput gain. However, when the LS length is 75 km and the hop count exceeds 5 only 6 of the 8 subcarriers can be practically used thus reducing the throughput of these solutions (yellow) to match that of the 4 subcarrier solutions (blue).

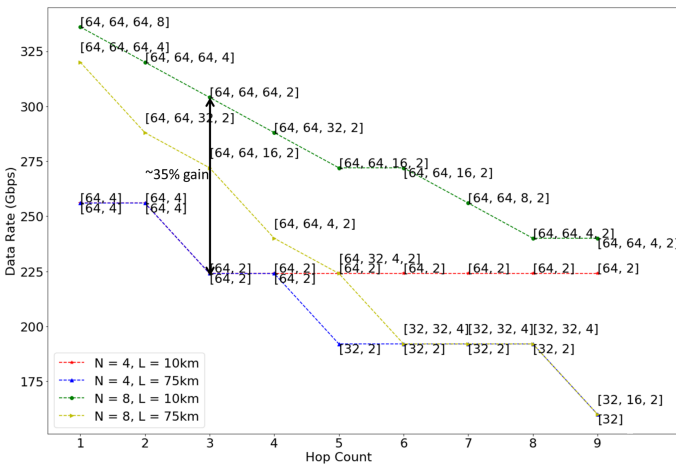


Fig. 11. Throughput versus hop count in superchannels using 4 and 8 subcarriers.

### C. Dynamic Bandwidth Allocation

Due to its fast and accurate estimation of the WSS filtering induced OSNR penalties, we believe that the proposed NN solution is quite useful in both network controllers and network planning tools. With the ability to quickly estimate the WSS filtering penalties incurred in any network path this technique has the potential to be used in highly dynamic scenarios, like assisting the network controller in concurrently choosing the best restoration path, flexible symbol rate, SCM channel configuration, and modulation format of a disrupted primary optical circuit.

## V. CONCLUSION

An artificial neural network (NN) comprising 12 features, two hidden layers of 256 neurons each, and one output is applied to estimate the OSNR penalties caused by cascaded WSS filtering in a DWDM metro network. These penalties are particularly relevant when designing and operating networks that make use of high-order modulation formats, flexible grid, an subcarrier multiplexing (SCM) technologies for improved spectral efficiency. The NN is used to estimate the fiber throughput gains that are achievable when transmitting with flexible symbol rates compared to the conventional fixed standard symbol rates. Another application of this NN is the selection of the optimal SCM superchannel configurations as a function of the network path hop count and length. Thanks to its sub-second run time this NN solution may find good applications in DWDM network controllers and planning tools.

## REFERENCES

- [1] (2020, Mar.) Cisco annual internet report (2018–2023) white paper. [Online]. Available: <https://www.cisco.com/c/en/us/solutions/collateral/executive-perspectives/annual-internet-report/white-paper-c11-741490.html>
- [2] R. Hui *et al.*, “Subcarrier multiplexing for high-speed optical transmission,” *Journal of Lightwave Technology*, vol. 20, no. 3, pp. 417–427, 2002.
- [3] M. Jinno, “Elastic optical networking: Roles and benefits in beyond 100-gb/s era,” *Journal of Lightwave Technology*, vol. 35, no. 5, pp. 1116–1124, 2017.
- [4] J. Pan *et al.*, “Osnr measurement comparison in systems with roadm filtering for flexible grid networks,” in *Proc. Optical Fiber Communications Conference and Exposition (OFC’ 18)*, 2018, pp. 1–3.
- [5] M. Qiu *et al.*, “Digital subcarrier multiplexing for fiber nonlinearity mitigation in coherent optical communication systems,” *Optics Express*, vol. 22, no. 15, pp. 18 770–18 777, Jul 2014.
- [6] T. Zhang *et al.*, “A comparative study on variable vs. fixed subchannel symbol rates with different modulation formats in wss filtering penalty-aware elastic optical networks,” in *Proc. International Conference on Transparent Optical Networks (ICTON’ 20)*, 2020, pp. 1–5.
- [7] S. Perrin. (2015, Mar.) Next-generation roadm architectures benefits. [Online]. Available: <https://www.fujitsu.com/us/Images/Fujitsu-NG-ROADM.pdf>
- [8] A. Morea *et al.*, “Impact of reducing channel spacing from 50ghz to 37.5ghz in fully transparent meshed networks,” in *Proc. Optical Fiber Communications Conference and Exposition (OFC’ 14)*, 2014, pp. 1–3.
- [9] J. Mata *et al.*, “Artificial intelligence (ai) methods in optical networks: A comprehensive survey,” *Optical Switching and Networking*, vol. 28, pp. 43 – 57, 2018.
- [10] J. Pan *et al.*, “Real-time roadm filtering penalty characterization and generalized precompensation for flexible grid networks,” *IEEE Photonics Journal*, vol. 9, no. 3, pp. 1–10, 2017.
- [11] C. Pulikkaseril *et al.*, “Spectral modeling of channel band shapes in wavelength selective switches,” *Optics Express*, vol. 19, no. 9, pp. 8458–8470, Apr 2011.
- [12] H. Simon, *Neural networks and learning machines*. New York: Prentice Hall, 2009.
- [13] (2012, Feb.) Spectral grids for wdm applications: Dwdm. [Online]. Available: <https://www.itu.int>
- [14] P. Poggiolini *et al.*, “The gn-model of fiber non-linear propagation and its applications,” *Journal of lightwave technology*, vol. 32, no. 4, pp. 694–721, 2013.
- [15] K. Sohn *et al.*, “A spare bandwidth sharing scheme based on network reliability,” *IEEE Transactions on Reliability*, vol. 54, no. 1, pp. 123–132, 2005.
- [16] A. Samadian *et al.*, “Two conflicting optimization problems in wdm networks: Minimizing spectrum fragmentation and maximizing quality of transmission,” in *Proc. IEEE International Conference on Communications (ICC’ 18)*, 2018, pp. 1–6.